Nowcasting Convection Occurrence from in-situ and Space-Borne Instability Predictors

P. Antonelli[(1)], A. Manzato [(2)], Stephen Tjemkes [(3)], Rolf Stuhlmann [(3)]

(1) Space Science Engineering Center

(2) OSservatorio MEteorologico Regionale (OSMER) ARPA Friuli Venezia Giulia

(3) European Organisation for the Exploitation of Meteorological Satellites

ITSC-XVIII, 21-27 March 2012, Toulouse

Hyperspectral mission goals

- **AIRS**: The Joint Center for Satellite Data Assimilation, established to accelerate the assimilation of satellite observations into operational weather forecast models, announced that significant improvement in forecast skill has been achieved with the assimilation of AIRS data. (http://airs.jpl.nasa.gov/mission/description/)
- The Infrared Atmospheric Sounding Interferometer **IASI** represents a significant advance in the quality of the measurements injected into models for understanding and making atmospheric forecasts. It uses particularly innovative technologies for a completely new European contribution to polar meteorology. (http://www.eumetsat.int/Home/Main/Satellites/Metop/Instruments/SP_20100531510474957l=en)
- **CrIS**: The Suomi National Polar-orbiting Partnership (Suomi NPP) mission represents a critical first step in building the next-generation Earth-observing satellite system that will collect data on both long-term climate change and short-term weather conditions. Suomi NPP is the result of a partnership between NASA, the National Oceanic and Atmospheric Administration, and the Department of Defense.
- **MTG-IRS**
  - Primary objective : To support regional and convective-scale NWP in Europe, through unprecedented detail on 3D fields of wind, temperature and humidity, at high vertical, horizontal and temporal resolution.
  - Other objectives: To support nowcasting and very-short range forecasting (VSRF), 3D fields of wind, temperature and humidity, ... and hence moisture convergence and convective instability, to help improve warnings of location and intensity of convective storms; To support global NWP - wind, temperature and humidity over Meteosat coverage area. (http://www.eumetsat.int/groups/pps/documents/document/pdf_mtg_ucw3_11.pdf)

Project

- **Aim**: to work with a forecaster on the use level 2 and level 1 products (temperature and water vapor vertical profiles) from high spectral resolution infrared sensors for short term forecasting of convection occurrence with emphasis on severe convection;
- **Phase**: currently in second year of activities (second phase);
- **Framework**: collaboration between EUMETSAT (supporting Institution), SSEC, and OSMER ARPA-FVG;
- **Approach**: develop a local short-forecast tool for convection occurrence, as detected by lightning observations, based on instability indices derived from rawinsondes and compare it to one based on instability indices and principal component scores derived from high spectral resolution infrared observations

Strategy

- Define occurrence of convective event, by setting threshold of 10 strikes to convert discrete distribution of lightning strikes into binary output event yes/no (1/0);

- Build Full Dataset with occurrence of convective event (yes/no) and values of all available predictors;

  - divide the full dataset into 2 subsets: 1) Total Set, to be used to build classifier; 2) Test Set, to be used for final evaluation of classifier capacity of prediction;

  - divide, in 12 different ways, Total Set into: 1) Training Set (75%); 2) Validation Set (25%); both to be used to sub-select the optimal predictors using Repeated Holdout Technique [Witten:2005]

Rawinsonde system

Phase I

Strategy

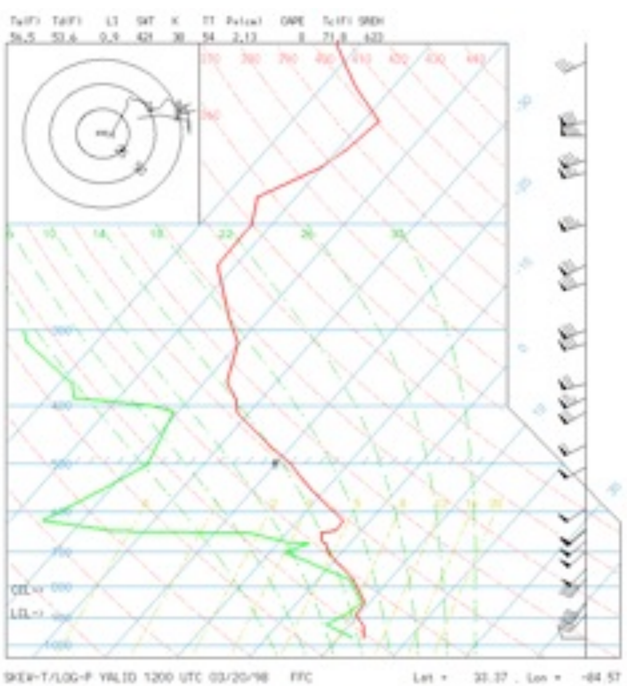

Rawinsonde system

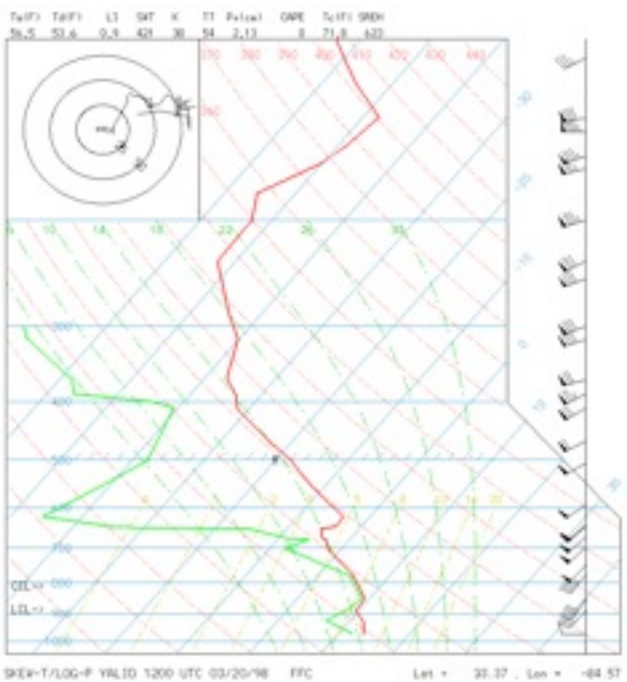

Ref.: PA/IIS/TR06/2011/01

P(JJJ) []	Julian day	SWEAT []	Severe weather threat
BOY []	Boyden index	MEL [%]	Melting level (parcel at 0°C)
BRI []	Bulk Richardson number	MLWu [ms^{-1}]	U component of midlevel wind (6 km)
BS850 [ms^{-1}]	Bulk Shear 850 hPa - 100 m	MLWv [ms^{-1}]	V component of midlevel wind (6 km)
CAP [^oC]	Maximum cap (as Θes difference)	MRH [%]	Mean relative humidity in the first 500 hPa
CAPE [J/kg]	Convective available potential energy	MaxBuo [K]	Maximum buoyancy
CIN [J/kg]	Convective inhibition	Mix [g/kg]	Most unstable parcel (MUP) mixing ratio
DT500 [^oC]	Difference of temperature at 500 hPa	PBL [m]	Planetary boundary layer estimated height
DTC [^oC]	Core difference of temperature	PWC [mm]	Precipitable water content of cloud
DownPotm [K]	Downdraft potential	PWE [mm]	Precipitable water content of environment
EHI []	Energy–helicity index	Rel_Hel [m^2s^{-2}]	Relative helicity
HD [cm]	Hail Diameter (derived from UpDr)	SWISS []	Stability and wind shear index for storms in Switzerland
HLJD [m]	High–levels (6–12 km) jet depth	Shear [s^{-1}]	Wind shear in the lowest 12 km
HLWu [ms^{-1}]	U component of high–levels (6–12 km) wind	Shear3 [s^{-1}]	Wind shear in the lowest 3 km
HLWv [ms^{-1}]	V component of high–levels (6–12 km) wind	ShowI [^oC]	Showalter index
HRH [%]	High–levels (500–300 hPa) relative humidity	Tbase [^oC]	Cloud-base (LCL) temperature
HEL [Jkg^{-1}]	Helicity	Thetae [K]	Most Unstable Parcel Θe
KI [^oC]	K index	Trop [m]	Tropopause height
LCL [m]	Lifting condensation level	UpDr [m/s]	"Core updraft" (parcel at -15°C)
LFC [m]	Level of free convection height	VFlux [$m^{-2}s^{-1}kg$]	Mean water vapor horizontal flux
LI [C]	Lifted index	VV [ms^{-1}]	Radiosonde ascensional vertical velocity
LLJD [m]	Low–levels (lowest 6 km) jet depth	VVstd [ms^{-1}]	Std dev of radiosonde vertical velocity
LLWu [ms^{-1}]	U component of low-level wind (0.5 km)	WBZ [m]	Environmental wet bulb zero height
LLWv [ms^{-1}]	V component of low-level wind (0.5 km)	b_PBL [cm/s2]	Mean buoyancy acceleration of the first 250 hPa
LRH [m]	Mean relative humidity in the first 250 hPa	h_MUP [m]	MUP height

6

Table 1.3: Instability Indices

Rawinsonde system

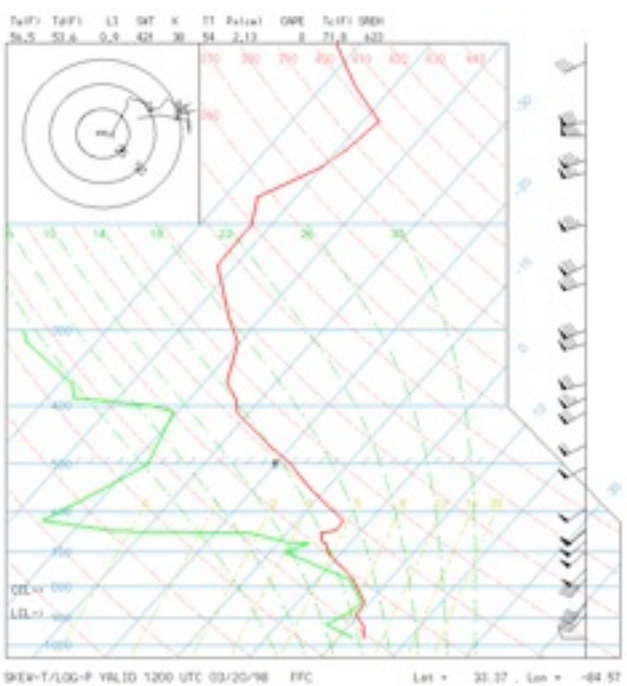

Ref.: PA/IIS/TR06/2011/01

P(JJJ) []	Julian day	SWEAT []	Severe weather threat
BOY []	Boyden index	MEL [%]	Melting level (parcel at 0°C)
BRI []	Bulk Richardson number	MLWu $[ms^{-1}]$	U component of midlevel wind (6 km)
BS850 $[ms^{-1}]$	Bulk Shear 850 hPa - 100 m	MLWv $[ms^{-1}]$	V component of midlevel wind (6 km)
CAP $[^oC]$	Maximum cap (as Θes difference)	MRH [%]	Mean relative humidity in the first 500 hPa
CAPE [J/kg]	Convective available potential energy	MaxBuo [K]	Maximum buoyancy
CIN [J/kg]	Convective inhibition	Mix [g/kg]	Most unstable parcel (MUP) mixing ratio
DT500 $[^oC]$	Difference of temperature at 500 hPa	PBL [m]	Planetary boundary layer estimated height
DTC $[^oC]$	Core difference of temperature	PWC [mm]	Precipitable water content of cloud
DownPotm [K]	Downdraft potential	PWE [mm]	Precipitable water content of environment
EHI []	Energy–helicity index	Rel_Hel $[m^2s^{-2}]$	Relative helicity
HD [cm]	Hail Diameter (derived from UpDr)	SWISS []	Stability and wind shear index for storms in Switzerland
HLJD [m]	High–levels (6–12 km) jet depth	Shear $[s^{-1}]$	Wind shear in the lowest 12 km
HLWu $[ms^{-1}]$	U component of high–levels (6–12 km) wind	Shear3 $[s^{-1}]$	Wind shear in the lowest 3 km
HLWv $[ms^{-1}]$	V component of high–levels (6–12 km) wind	ShowI $[^oC]$	Showalter index
HRH [%]	High–levels (500–300 hPa) relative humidity	Tbase $[^oC]$	Cloud-base (LCL) temperature
HEL $[Jkg^{-1}]$	Helicity	Thetae [K]	Most Unstable Parcel Θe
KI $[^oC]$	K index	Trop [m]	Tropopause height
LCL [m]	Lifting condensation level	UpDr [m/s]	"Core updraft" (parcel at -15°C)
LFC [m]	Level of free convection height	VFlux $[m^{-2}s^{-1}kg]$	Mean water vapor horizontal flux
LI [C]	Lifted index	VV $[ms^{-1}]$	Radiosonde ascensional vertical velocity
LLJD [m]	Low–levels (lowest 6 km) jet depth	VVstd $[ms^{-1}]$	Std dev of radiosonde vertical velocity
LLWu $[ms^{-1}]$	U component of low-level wind (0.5 km)	WBZ [m]	Environmental wet bulb zero height
LLWv $[ms^{-1}]$	V component of low-level wind (0.5 km)	b_PBL [cm/s2]	Mean buoyancy acceleration of the first 250 hPa
LRH [m]	Mean relative humidity in the first 250 hPa	h_MUP [m]	MUP height

6

Table 1.3: Instability Indices

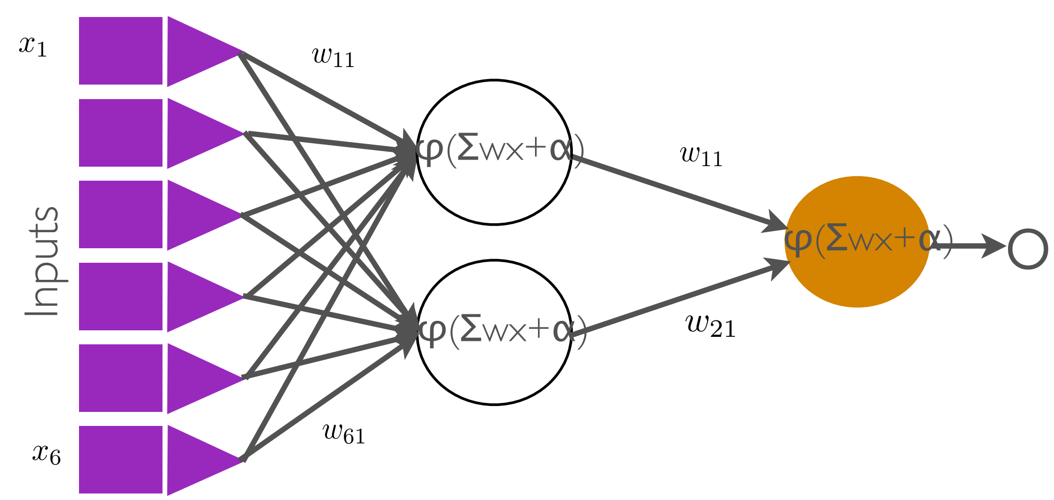

Rawinsonde system

Phase I

Strategy

- Predictors: 50 instability indices derived from rawinsondes launched in Milano and Udine at 11:00 UTC;
- convection Occurrence: events with more than 10 lightning strikes within 11:00 and 17:00 UTC for time period April - October) over the Po Valley;
- subset of optimal predictors are chosen by a forward selection algorithm (based on Artificial Neural Networks, namely single layer, feedforward network trained with backpropagation [Manzato:2004, Manzato-2007]);

- once optimal subset of predictors is identified, final ANN architecture is chosen among different candidates (different numbers of hidden neurons in hidden layer) as one with lowest combined CEE on Total set (Training + Validation);

Results over Milano

Phase I | Raob Results

- During input selection phase (forward selection algorithm) only Total set was used, it included 957 cases and was used to train different ANN candidates. While to select best architecture (hidden neurons) for the prediction system (ANN) also consistency between the results obtained on the Total and on the Test sets (of 328 cases) was taken into account. The architecture chosen was with 8 inputs (KI LLWv HD MEL ShowI CAP SWISS), 2 neurons on the hidden layer, and 1 output.

TRAINING: Application of the ANN on the Total set led to a Total **CEE** of **0.303**, while applying the probability threshold (0.28) on the continuous ANN output led to the following contingency table:

TOTAL	Event (Y)	Event (N)
Prediction: YES	186	11
Prediction: NO	40	620

TOTAL	POD	HIT	FAR	POFD	**PSS**
Score	0.82	0.84	0.37	0.15	**0.67**

TESTING: Applying ANN on Test set led to a Test **CEE** of **0.332**, while applying the probability threshold (0.28) on the continuous ANN output led to the following contingency table:

TEST	Event (Y)	Event (N)
Prediction: YES	72	48
Prediction: NO	14	194

TEST	POD	HIT	FAR	POFD	**PSS**
Score	0.83	0.81	0.4	0.19	**0.64**

Retrieval system

Phase I

Strategy

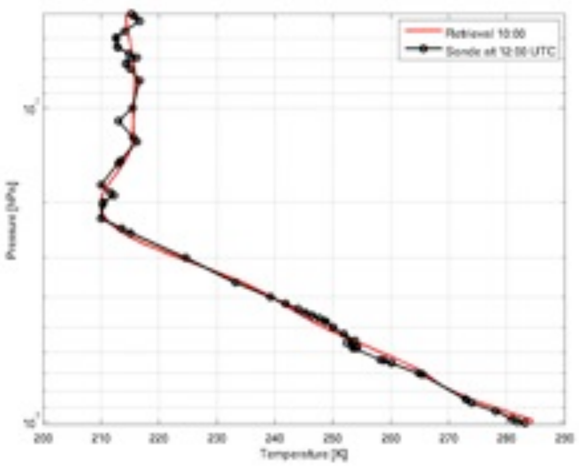

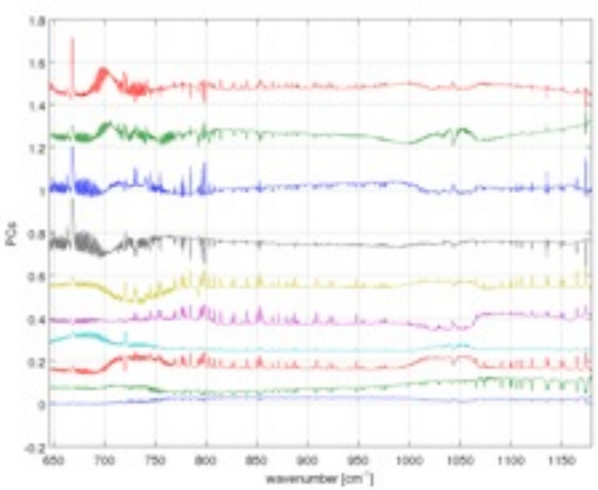

Retrieval system

Phase I

Strategy

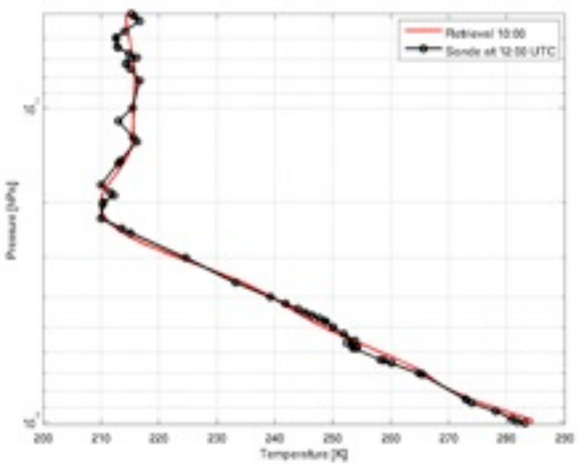

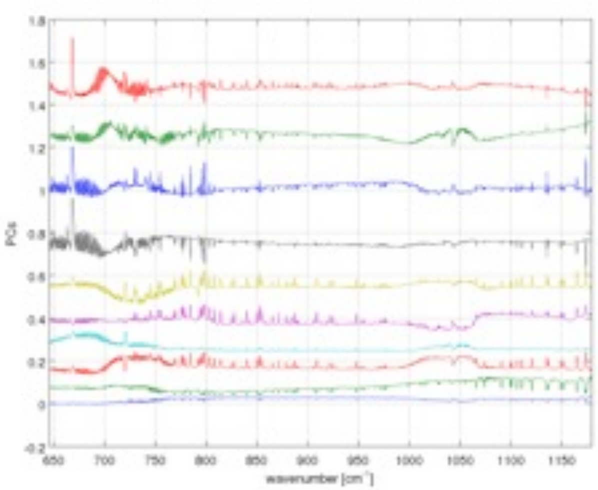

P(JJJ) []	Julian day	SWEAT []	Severe weather threat
BOY []	Boyden index	MEL [%]	Melting level (parcel at 0°C)
BRI []	Bulk Richardson number	MLWu [ms^{-1}]	U component of midlevel wind (6 km)
BS850 [ms^{-1}]	Bulk Shear 850 hPa - 100 m	MLWv [ms^{-1}]	V component of midlevel wind (6 km)
CAP [^oC]	Maximum cap (as Θes difference)	MRH [%]	Mean relative humidity in the first 500 hPa
CAPE [J/kg]	Convective available potential energy	MaxBuo [K]	Maximum buoyancy
CIN [J/kg]	Convective inhibition	Mix [g/kg]	Most unstable parcel (MUP) mixing ratio
DT500 [^oC]	Difference of temperature at 500 hPa	PBL [m]	Planetary boundary layer estimated height
DTC [^oC]	Core difference of temperature	PWC [mm]	Precipitable water content of cloud
DownPotm [K]	Downdraft potential	PWE [mm]	Precipitable water content of environment
EHI []	Energy–helicity index	Rel_Hel [m^2s^{-2}]	Relative helicity
HD [cm]	Hail Diameter (derived from UpDr)	SWISS []	Stability and wind shear index for storms in Switzerland
HLJD [m]	High–levels (6–12 km) jet depth	Shear [s^{-1}]	Wind shear in the lowest 12 km
HLWu [ms^{-1}]	U component of high–levels (6–12 km) wind	Shear3 [s^{-1}]	Wind shear in the lowest 3 km
HLWv [ms^{-1}]	V component of high–levels (6–12 km) wind	ShowI [^oC]	Showalter index
HRH [%]	High–levels (500–300 hPa) relative humidity	Tbase [^oC]	Cloud-base (LCL) temperature
HEL [Jkg^{-1}]	Helicity	Thetae [K]	Most Unstable Parcel Θe
KI [^oC]	K index	Trop [m]	Tropopause height
LCL [m]	Lifting condensation level	UpDr [m/s]	“Core updraft” (parcel at -15°C)
LFC [m]	Level of free convection height	VFlux [$m^{-2}s^{-1}kg$]	Mean water vapor horizontal flux
LI [C]	Lifted index	VV [ms^{-1}]	Radiosonde ascensional vertical velocity
LLJD [m]	Low–levels (lowest 6 km) jet depth	VVstd [ms^{-1}]	Std dev of radiosonde vertical velocity
LLWu [ms^{-1}]	U component of low-level wind (0.5 km)	WBZ [m]	Environmental wet bulb zero height
LLWv [ms^{-1}]	V component of low-level wind (0.5 km)	b_PBL [cm/s2]	Mean buoyancy acceleration of the first 250 hPa
LRH [m]	Mean relative humidity in the first 250 hPa	h_MUP [m]	MUP height

Table 1.3: Instability Indices

+PC scores

Retrieval system

Phase I | **Strategy**

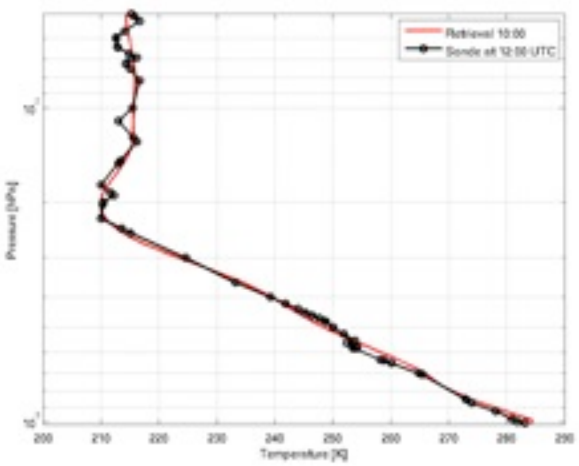

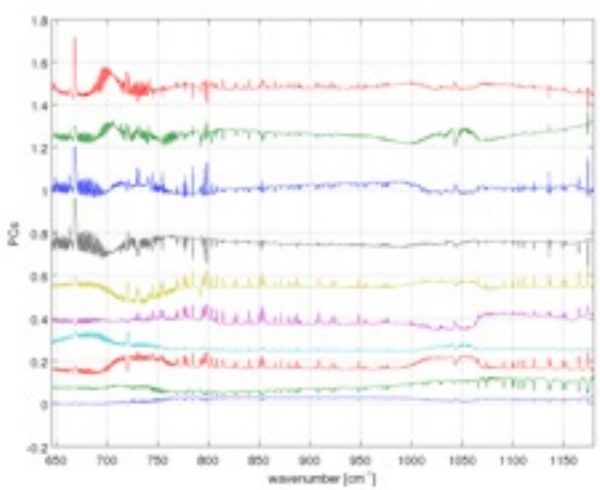

Ref.: PA/IIS/TR06/2011/01

P(JJJ) []	Julian day	SWEAT []	Severe weather threat
BOY []	Boyden index	MEL [%]	Melting level (parcel at 0°C)
BRI []	Bulk Richardson number	MLWu [ms^{-1}]	U component of midlevel wind (6 km)
BS850 [ms^{-1}]	Bulk Shear 850 hPa - 100 m	MLWv [ms^{-1}]	V component of midlevel wind (6 km)
CAP [^oC]	Maximum cap (as Θes difference)	MRH [%]	Mean relative humidity in the first 500 hPa
CAPE [J/kg]	Convective available potential energy	MaxBuo [K]	Maximum buoyancy
CIN [J/kg]	Convective inhibition	Mix [g/kg]	Most unstable parcel (MUP) mixing ratio
DT500 [^oC]	Difference of temperature at 500 hPa	PBL [m]	Planetary boundary layer estimated height
DTC [^oC]	Core difference of temperature	PWC [mm]	Precipitable water content of cloud
DownPotm [K]	Downdraft potential	PWE [mm]	Precipitable water content of environment
EHI []	Energy–helicity index	Rel_Hel [m^2s^{-2}]	Relative helicity
HD [cm]	Hail Diameter (derived from UpDr)	SWISS []	Stability and wind shear index for storms in Switzerland
HLJD [m]	High–levels (6–12 km) jet depth	Shear [s^{-1}]	Wind shear in the lowest 12 km
HLWu [ms^{-1}]	U component of high–levels (6–12 km) wind	Shear3 [s^{-1}]	Wind shear in the lowest 3 km
HLWv [ms^{-1}]	V component of high–levels (6–12 km) wind	ShowI [^oC]	Showalter index
HRH [%]	High–levels (500–300 hPa) relative humidity	Tbase [^oC]	Cloud-base (LCL) temperature
HEL [Jkg^{-1}]	Helicity	Thetae [K]	Most Unstable Parcel Θe
KI [^oC]	K index	Trop [m]	Tropopause height
LCL [m]	Lifting condensation level	UpDr [m/s]	"Core updraft" (parcel at -15°C)
LFC [m]	Level of free convection height	VFlux [$m^{-2}s^{-1}kg$]	Mean water vapor horizontal flux
LI [C]	Lifted index	VV [ms^{-1}]	Radiosonde ascensional vertical velocity
LLJD [m]	Low–levels (lowest 6 km) jet depth	VVstd [ms^{-1}]	Std dev of radiosonde vertical velocity
LLWu [ms^{-1}]	U component of low-level wind (0.5 km)	WBZ [m]	Environmental wet bulb zero height
LLWv [ms^{-1}]	V component of low-level wind (0.5 km)	b_PBL [cm/s2]	Mean buoyancy acceleration of the first 250 hPa
LRH [m]	Mean relative humidity in the first 250 hPa	h_MUP [m]	MUP height

6

Table 1.3: Instability Indices

+PC scores

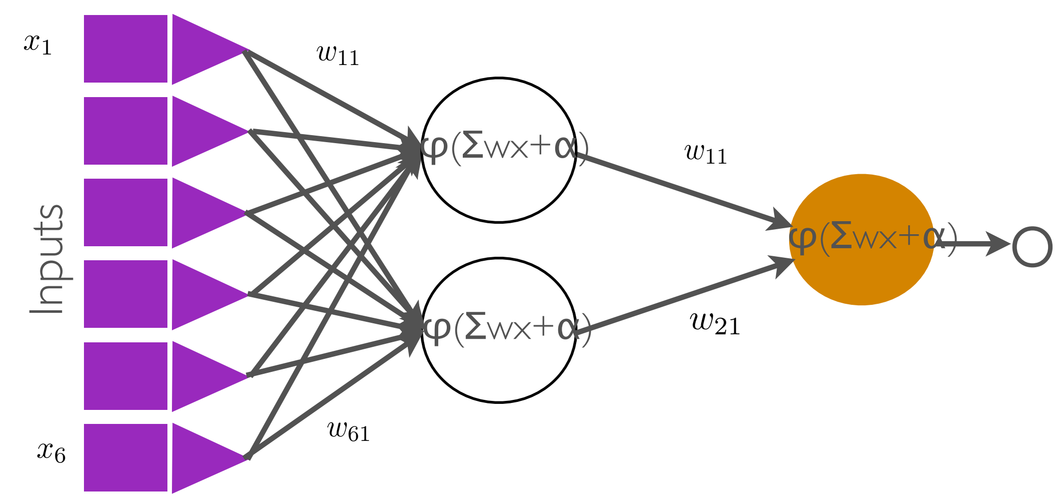

Key elements for using retrievals to derive instability indices

- how to perform quality control on retrieved profiles
  - spectral residuals;
  - comparison with available rawinsondes;
- how to combine retrievals to characterize the airmasses
  - derive indices from average of available retrievals for a given overpass;
  - derive indices from single retrieval;

Spectral Validation

Key Elements | Residual QC

- Retrieval residuals were calculated by comparing radiances simulated off retrieved profiles using the OSS forward model, with observed reconstructed radiances;
- Reconstructed radiances were preferred to original observations because of the noise filtering properties of PCA [Antonelli:2004] compression;
- Residuals obtained were averaged in 5 spectral regions and were compared (in terms of Brightness Temperature) to the mean observation error (in BT) used in the retrieval process;
- The 5 spectral regions were selected to guarantee that observations were properly fit in the 14 µm carbon dioxide band (accuracy of vertical profile of temperature), in the 9.7 µm ozone band (accuracy of Ozone vertical distribution), in the 6.7 µm water vapor band (accuracy of vertical distribution of water vapor), in the 11-12 µm window (accuracy of surface emissivity and surface temperature), and in the 8.6 µm band (accuracy of surface emissivity and surface temperature, presence of high load of aerosols and/or presence of thin cirrus clouds);
- Only retrievals with average residuals smaller than average observation error, in all 5 bands were considered spectrally successful.

	CO_2	Win	O_3	Win 2	H_2O	Total
Range in cm^{-1}	670-775	775-990	990-1070	1090-1120	1420-2100	670-2200

Spectral validation

Key Elements

Residual QC

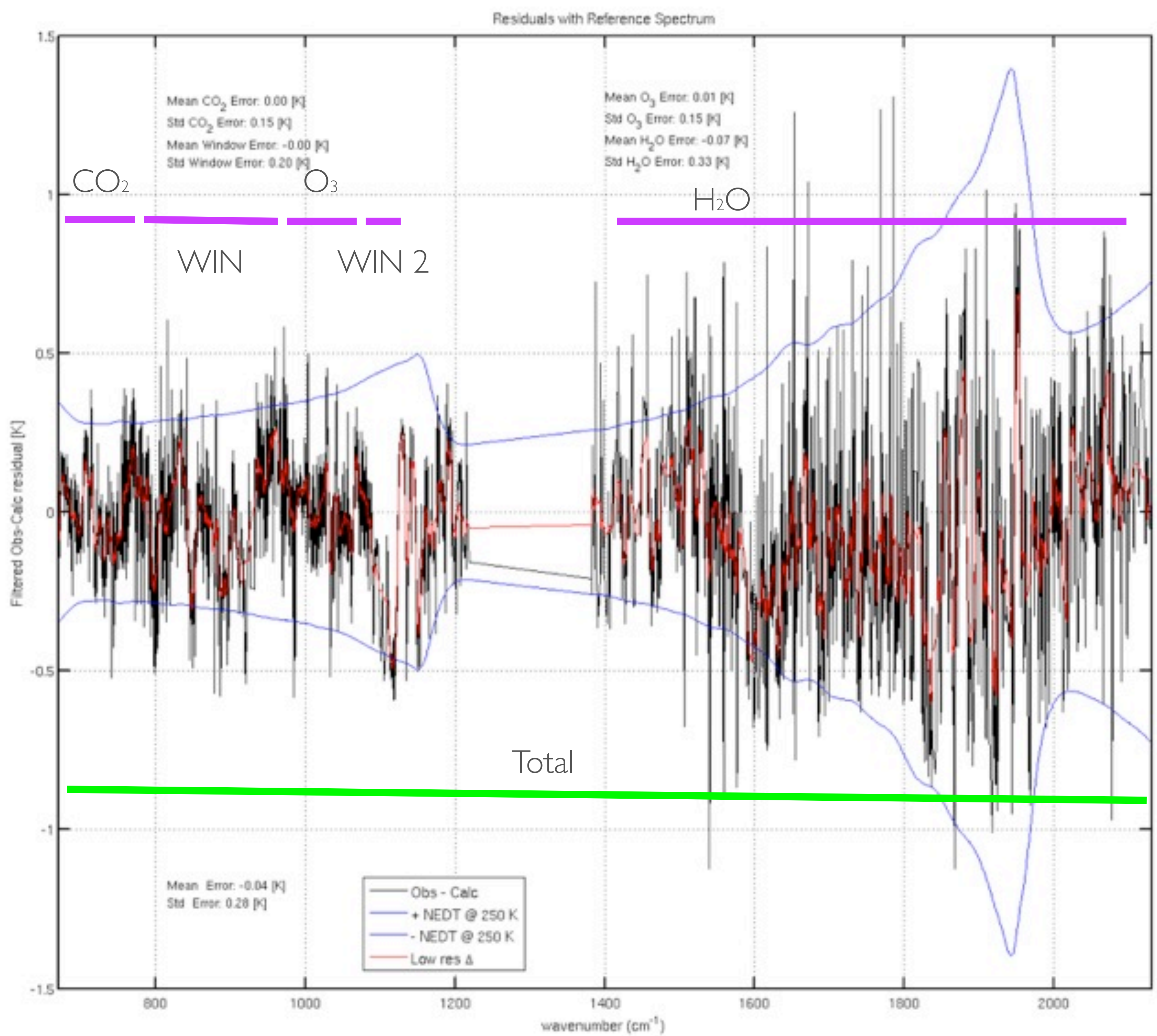

Characterization of the airmass using retrievals

Key Elements | Event Selection

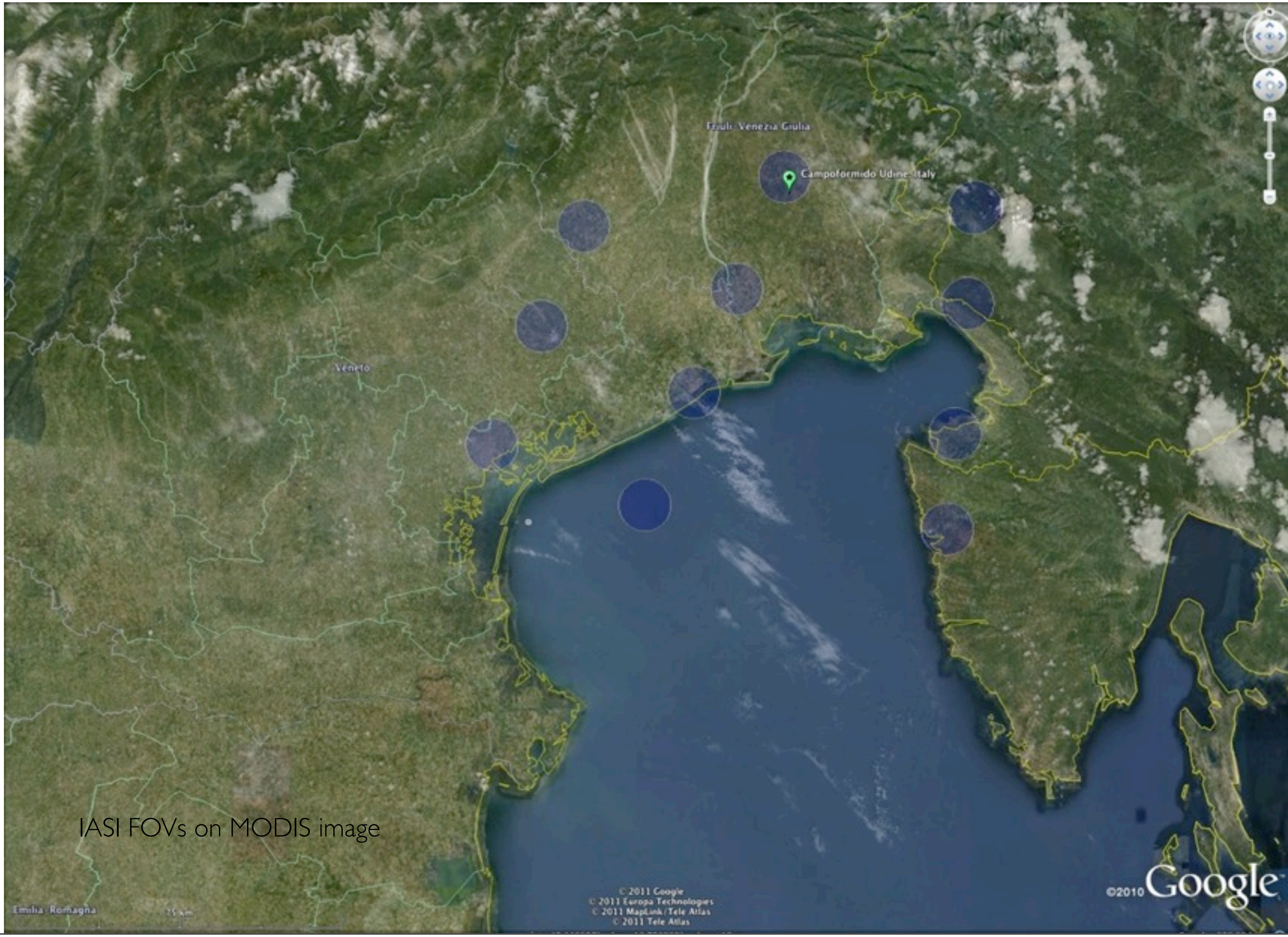

Successful retrieval

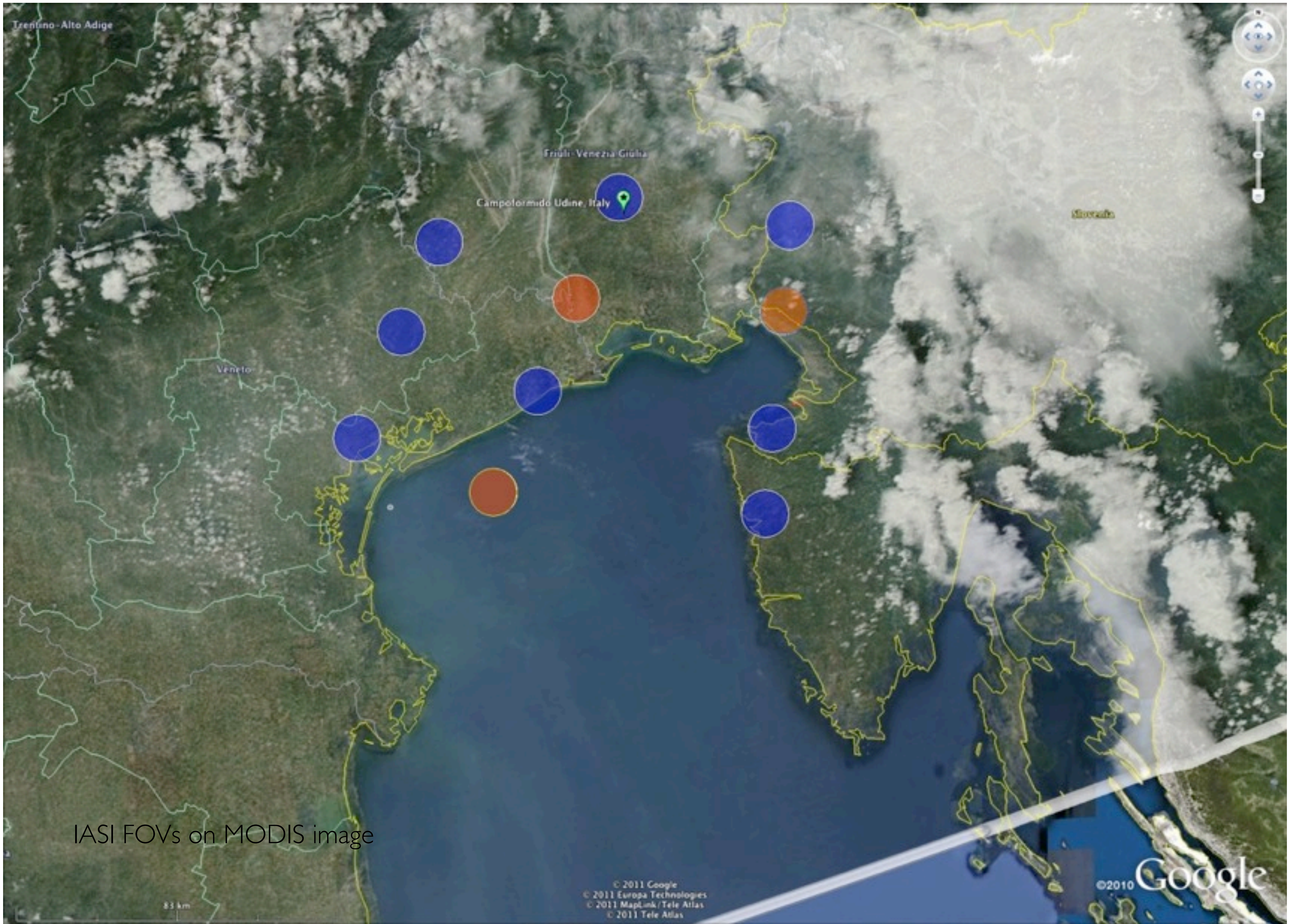

Combination strategy

Key Elements | Event Selection

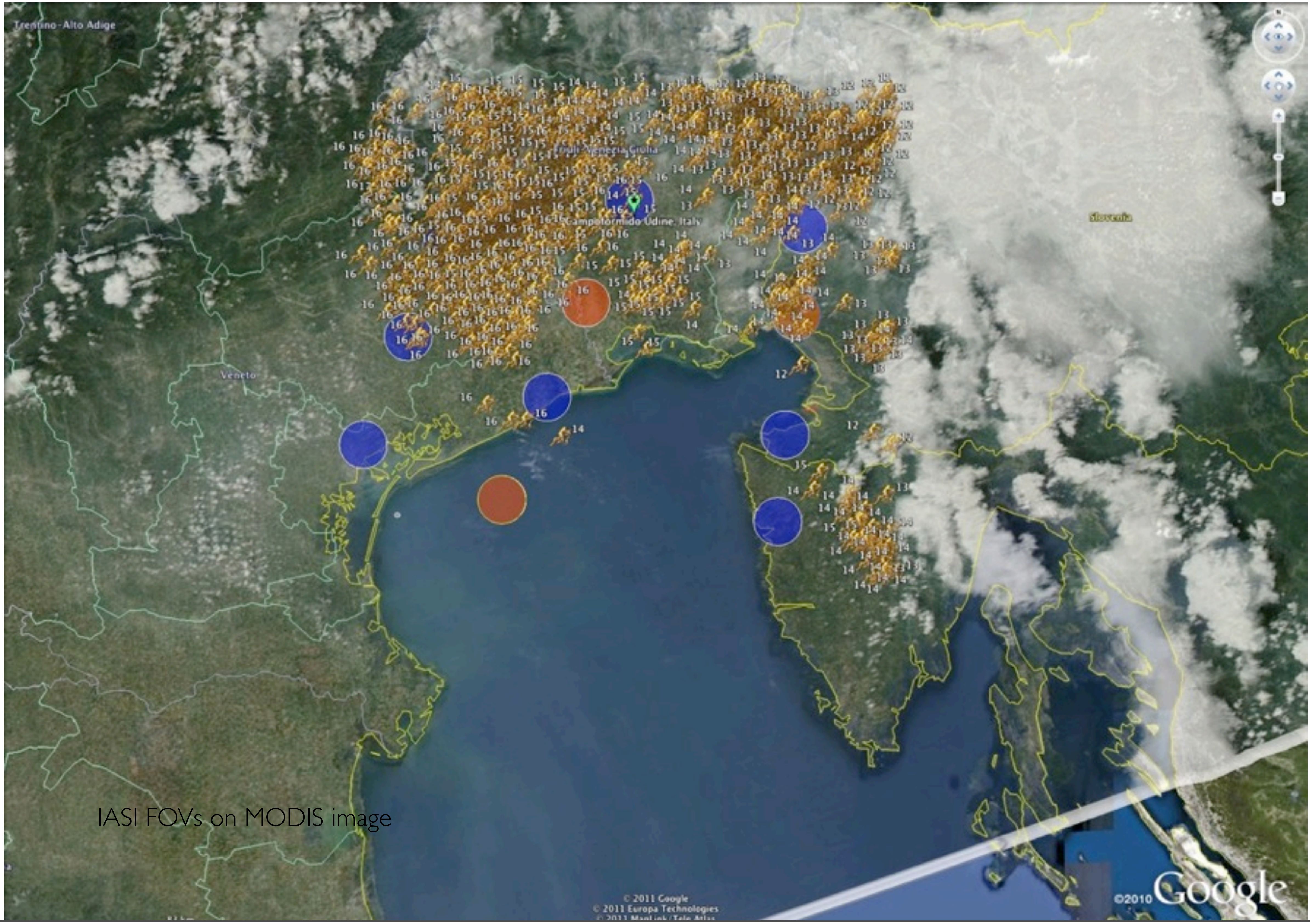

Combination strategy

Key Elements

Event Selection

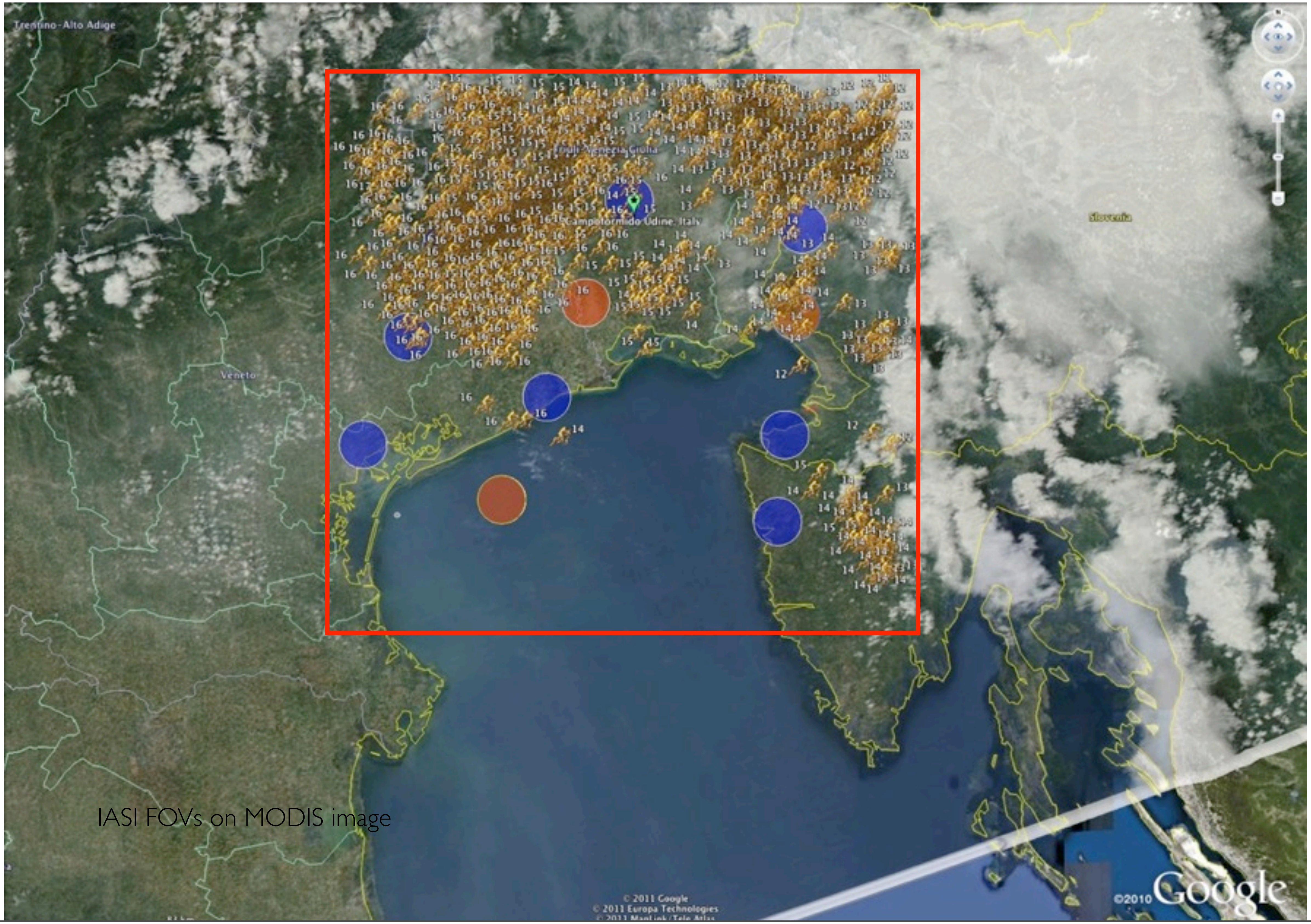

Combination strategy

Key Elements | Event Selection

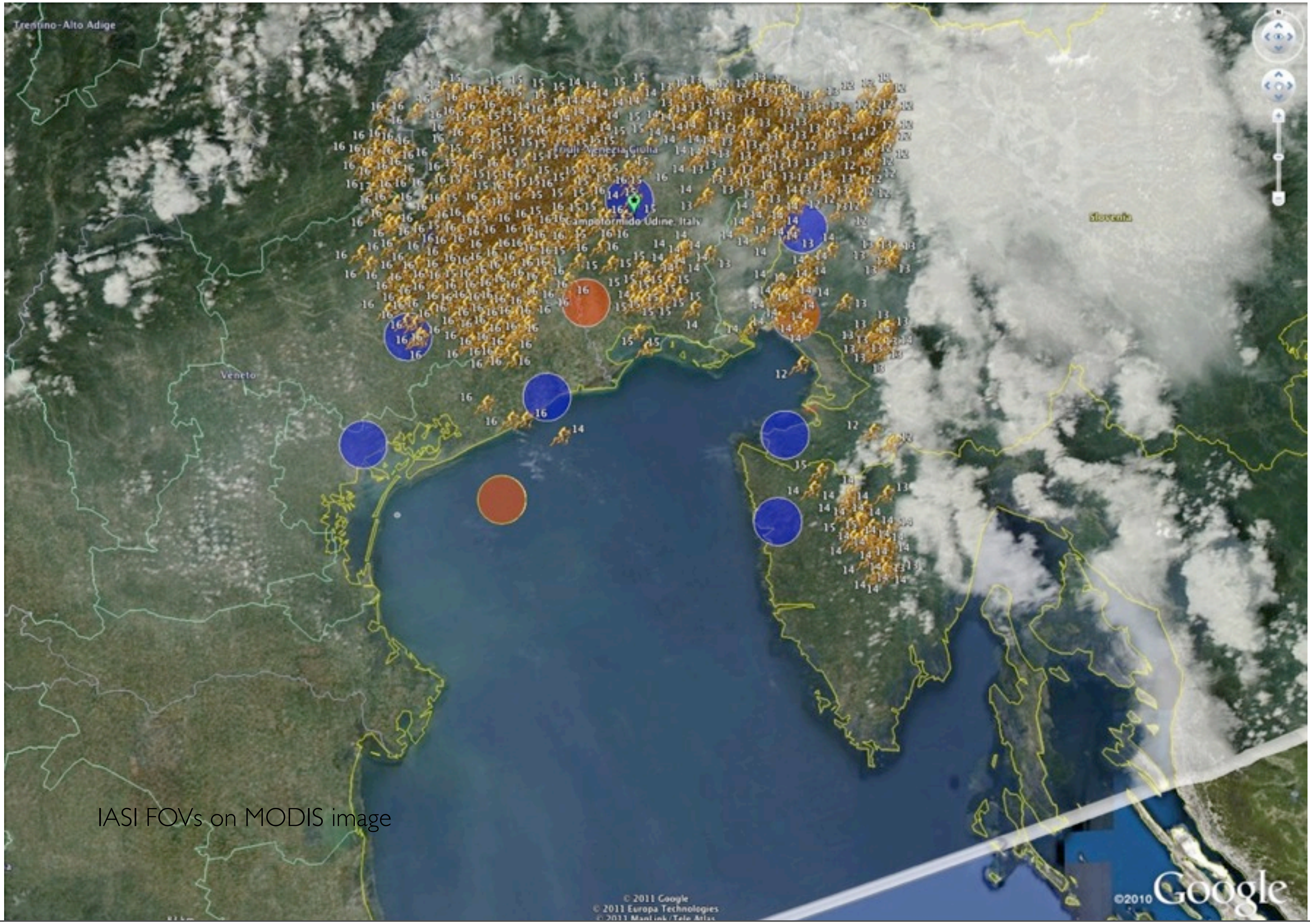

ISSUES:
Retrievals (09:00UTC) - Rawinsondes (11:00 UTC) T

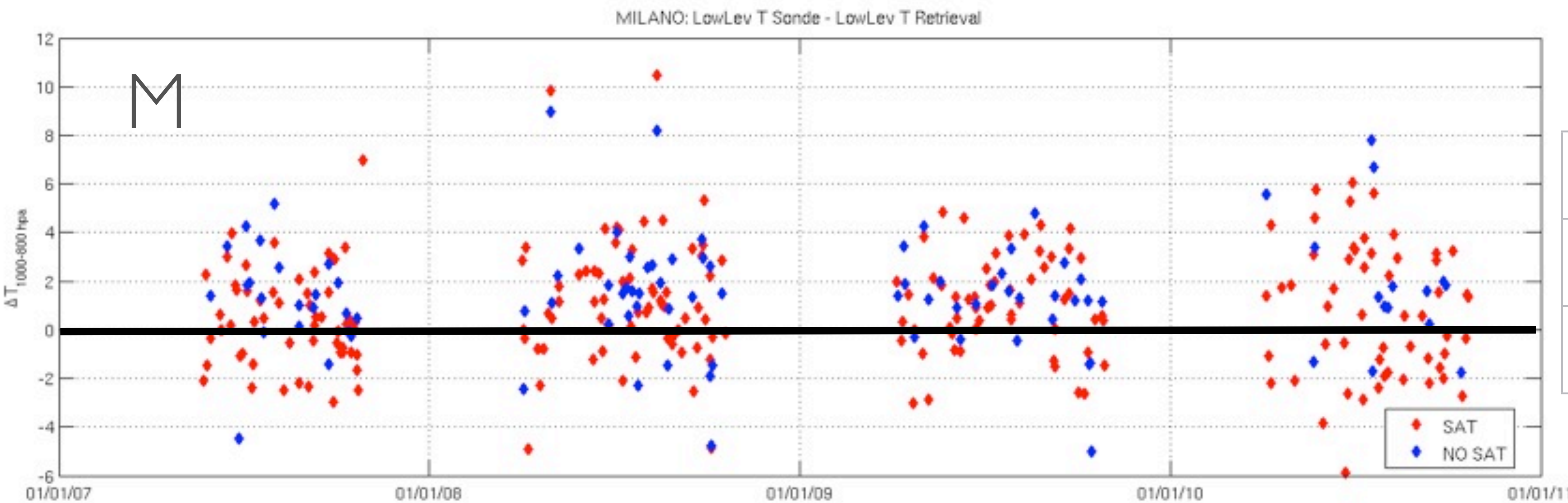

M	NS	S	Tot
T [K]	**1.4**	**0.8**	**1.1**
MR [g/kg]	-0.5	-1.3	-0.9

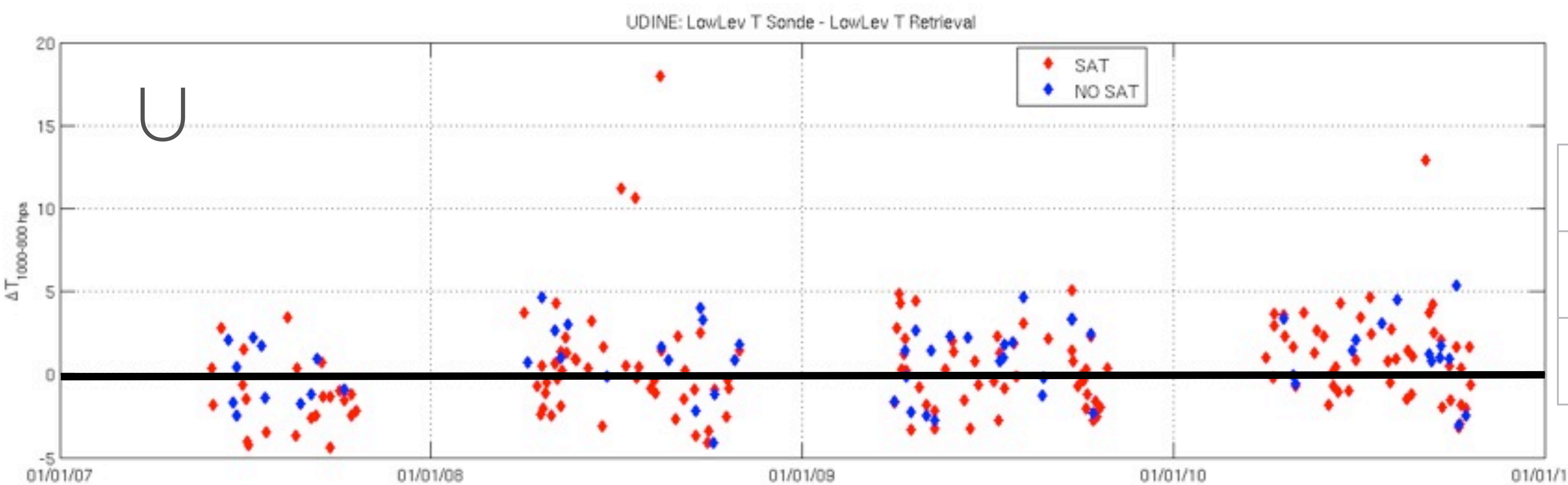

U	NS	S	Tot
T [K]	**0.74**	**0.4**	**0.57**
MR [g/kg]	-1.6	-2.0	-1.8

ISSUES:
Retrievals (09:00 UTC) - Rawinsondes (11:00 UTC) MR

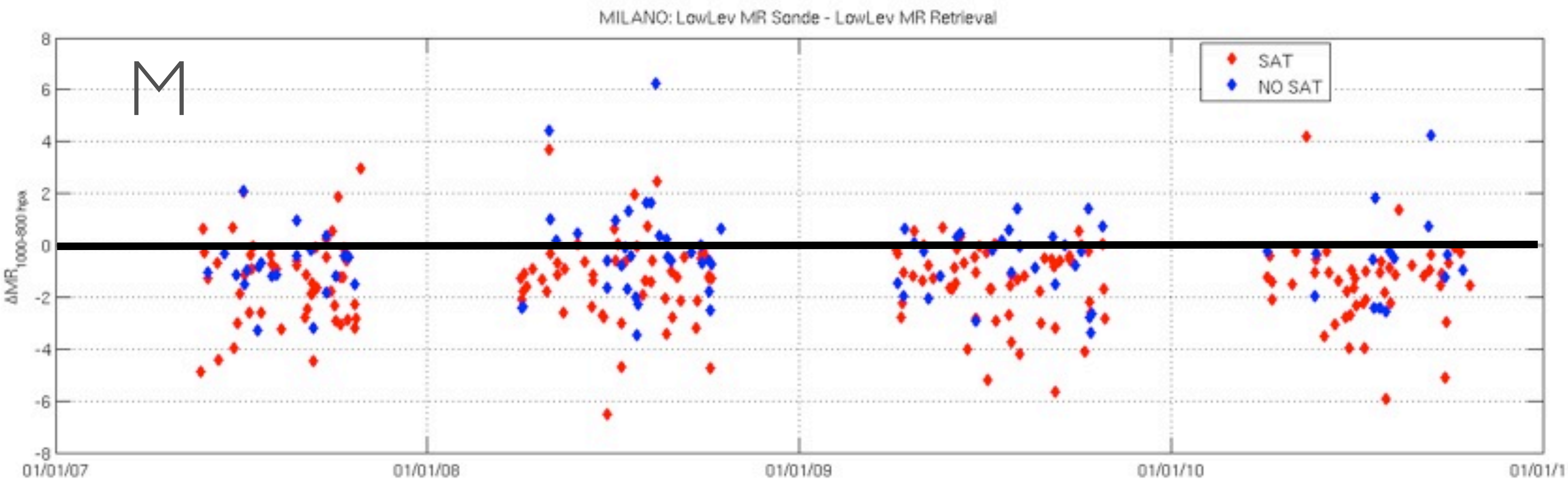

M	NS	S	Tot
T [K]	1.4	0.8	1.1
MR [g/kg]	**-0.5**	**-1.3**	**-0.9**

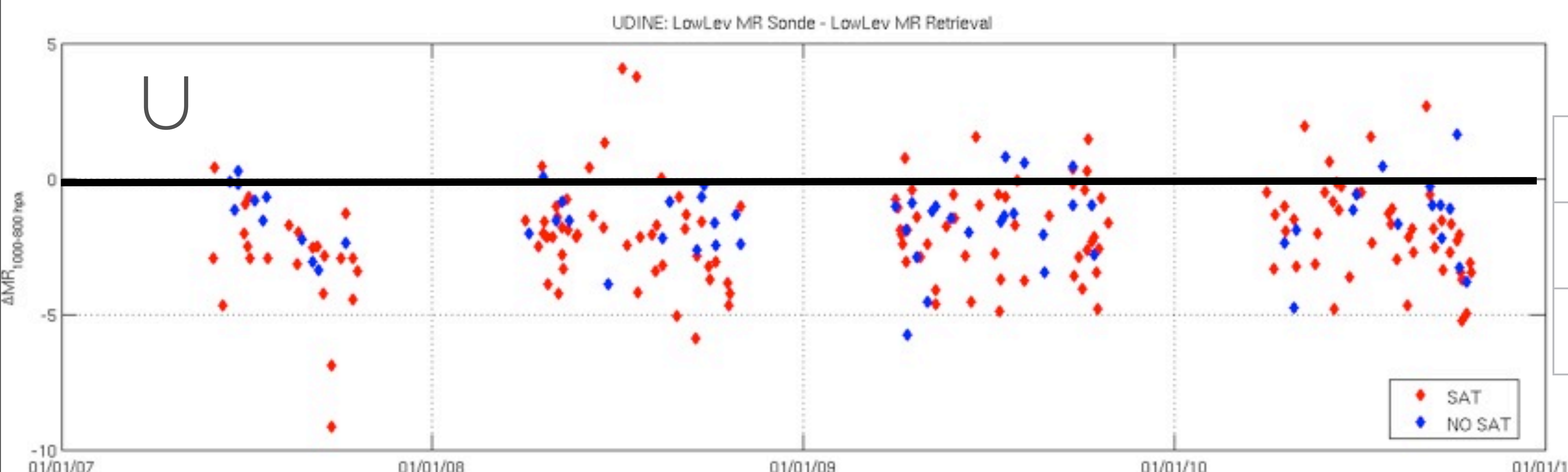

U	NS	S	Tot
T [K]	0.74	0.4	0.57
MR [g/kg]	**-1.6**	**-2.0**	**-1.8**

Retrievals

Phase I

Ret. Results

- By focusing on single area of interest, it was possible to generate ANN trained on a IASI dataset twice as large as the Full IASI Set. In this case the event occurrence was defined by at least 3 lightning strikes. Best ANN-inputs were **KI**, **PCS LW 12**, **PCS LW 17**. The best ANN, a 3 input, 1 hidden neuron.

TRAINING: Application of the ANN on the Total set led to a Total **CEE** of **0.40**, on 242 cases, while applying the probability threshold (0.29) on the continuous ANN output led to the following contingency table:

TOTAL	Event (Y)	Event (N)
Prediction: YES	36	41
Prediction: NO	25	140

TOTAL	POD	HIT	FAR	POFD	**PSS**
Score	0.59	0.73	0.53	0.23	**0.36**

TESTING: Applying ANN on Test set led to a Test **CEE** of **0.42**, on 89 cases, while applying the probability threshold (0.28) on the continuous ANN output led to the following contingency table:

TEST	Event (Y)	Event (N)
Prediction: YES	17	13
Prediction: NO	6	53

TEST	POD	HIT	FAR	POFD	**PSS**
Score	0.74	0.79	0.43	0.2	**0.49**

Conclusions on first experiment

- Rawinsondes launched in Milano Linate, and Udine Campoformido between 2004-2010 were used to produce sets of 50 instability indices
  - application of the network to the Total (or Training) and Test sets led to CEE di 0.303 and 0.332 respectively. By setting the discretization threshold (event: YES/NO) to 0.28 the ANN produced two contingency tables for Total and Test associated to PSS scores of 0.67 and 0.64 respectively;
- Retrievals over single area of interest led to prediction PSS score on the test set reached value of 0.49, indicating that nowcasting of convection by IASI data over individual (smaller) areas is feasible but not adequate;
- Principal componets were selected among best predictors for the IASI-based system;
- Poor results obtained in generalization for IASI data and products, were found to be mostly dependent:
  - on limited size of the IASI database (available retrievals in clear sky conditions);
  - general tendency of the retrievals to overestimate low level water vapor, which led to overestimation of the atmospheric instability, was found and should be further investigated;

Second Phase of the project

- Improving retrievals
  - changes in the apriori climatology;
  - estimation of the model error;
  - improved surface emissivity retrieval (bug fix);
- Increasing number of available observations
  - changing combination strategy
  - applying the system to AIRS retrievals over Udine (2001-2011)

Improved retrievals
Retrievals (09:00 UTC) - Rawinsondes (11:00 UTC) T

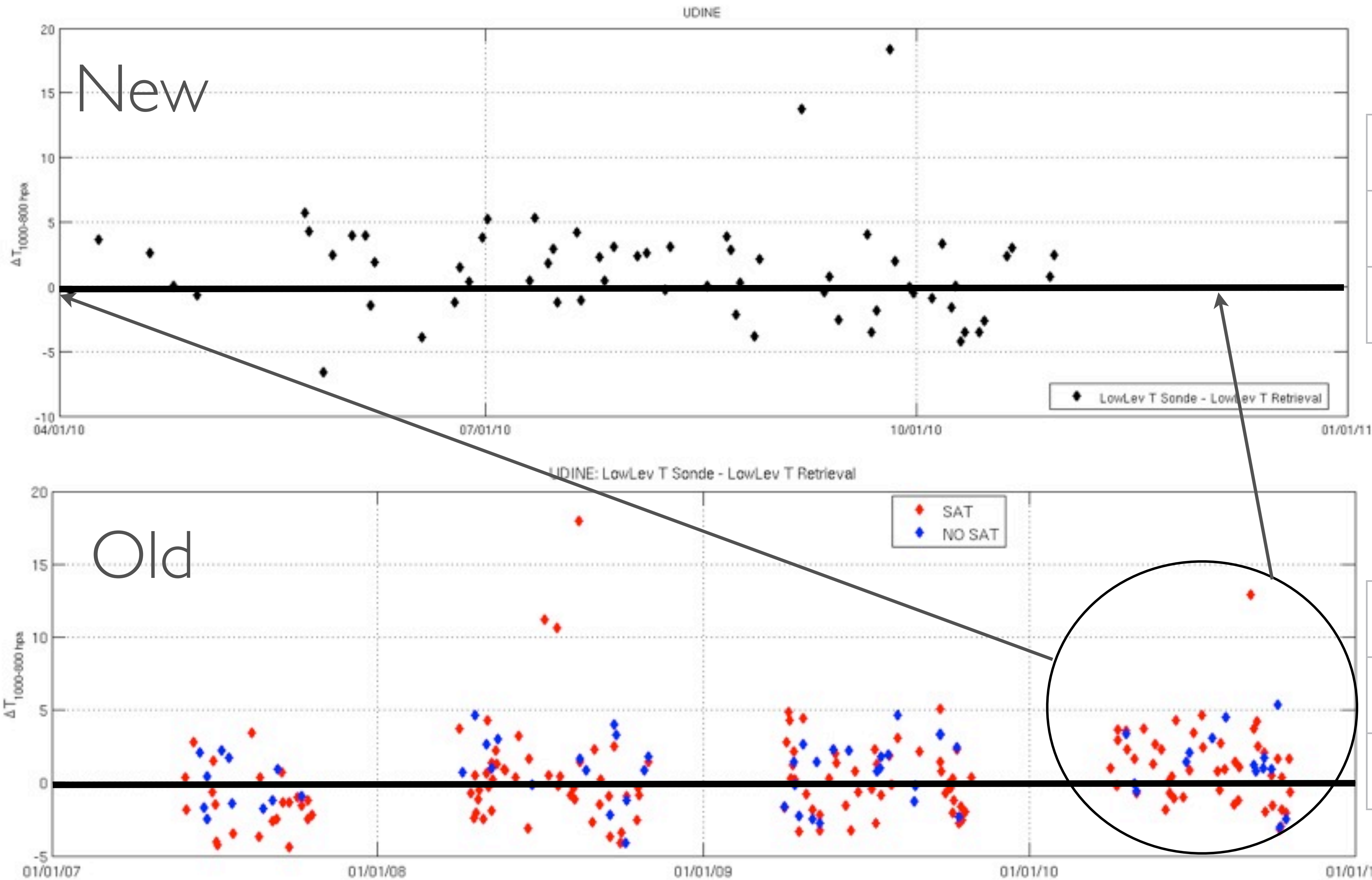

M	Tot
T [K]	**1.28**
MR [g/kg]	-0.7

U	NS	S	Tot
T [K]	**0.74**	**0.4**	**0.57**
MR [g/kg]	-1.6	-2.0	-1.8

Improved retrievals
Retrievals (09:00 UTC) - Rawinsondes (11:00 UTC) MR

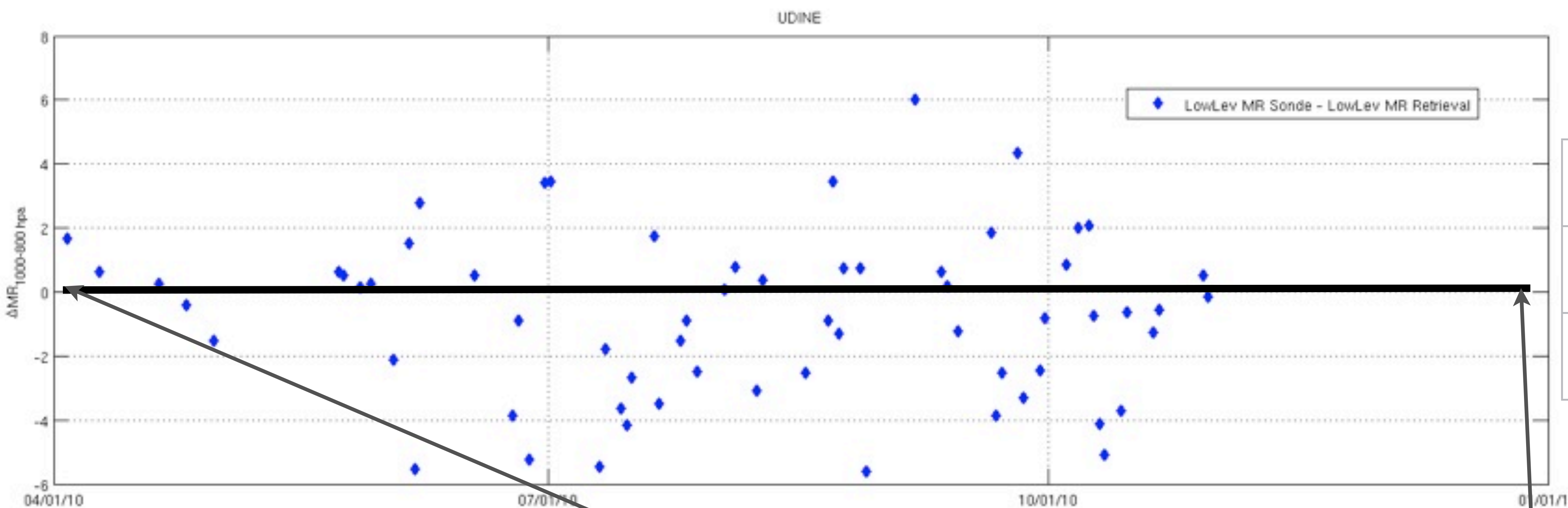

M	Tot
T [K]	1.28
MR [g/kg]	**-0.73**

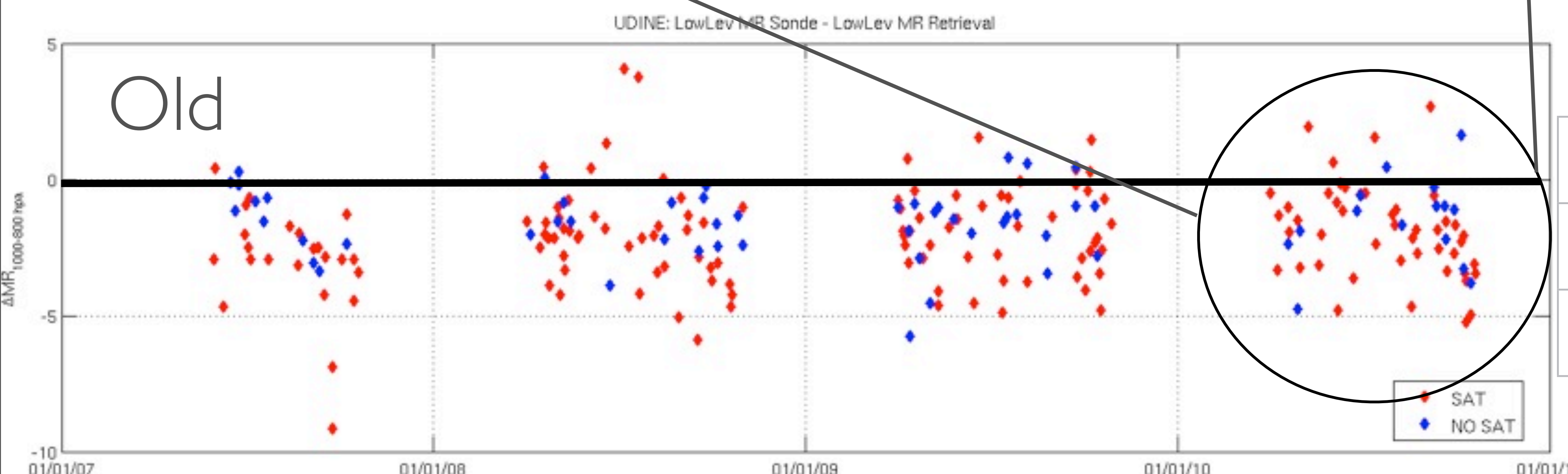

U	NS	S	Tot
T [K]	0.74	0.4	0.57
MR [g/kg]	**-1.6**	**-2.0**	**-1.8**

New combination strategy

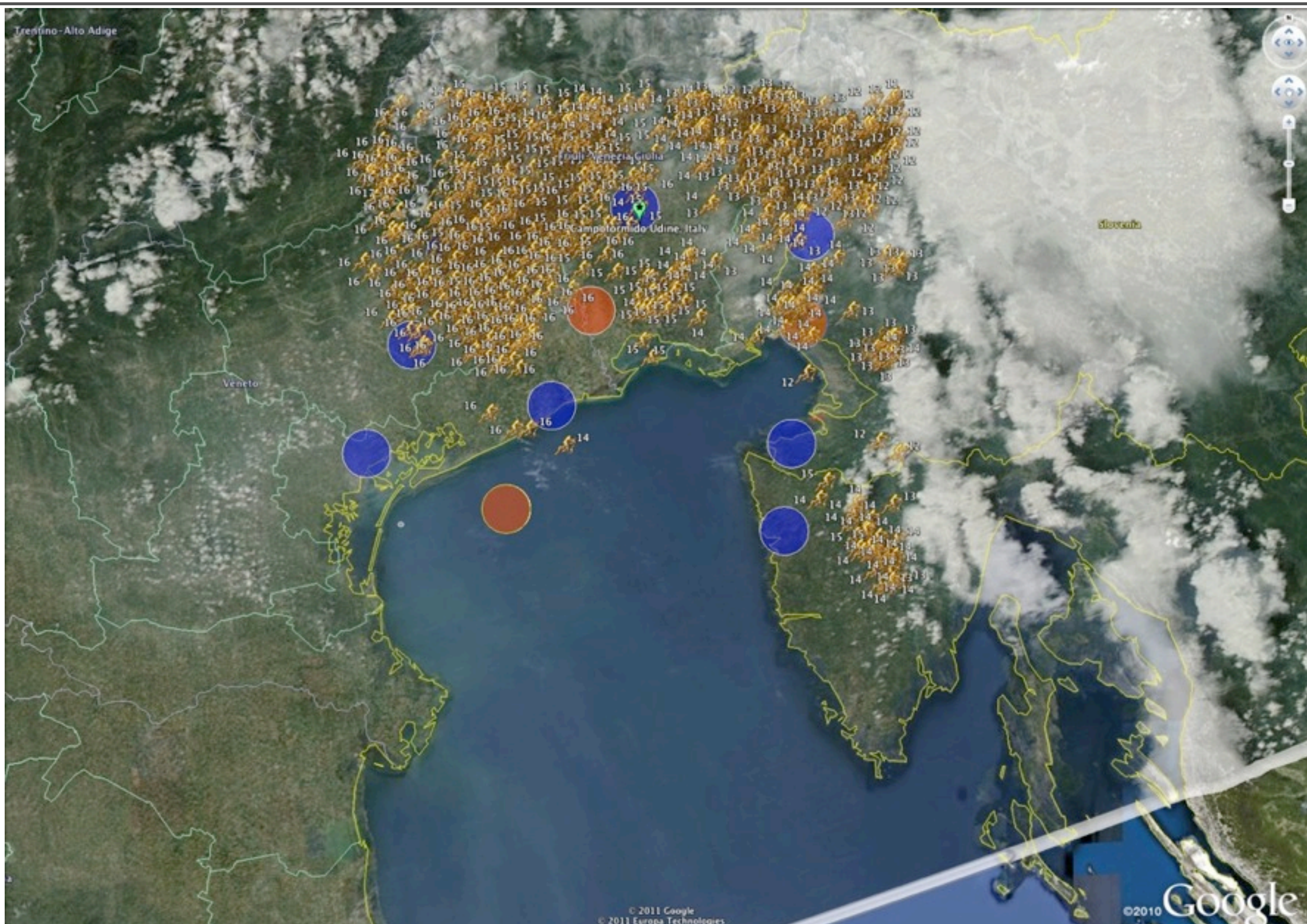

New combination strategy

Phase II

Improvemnts

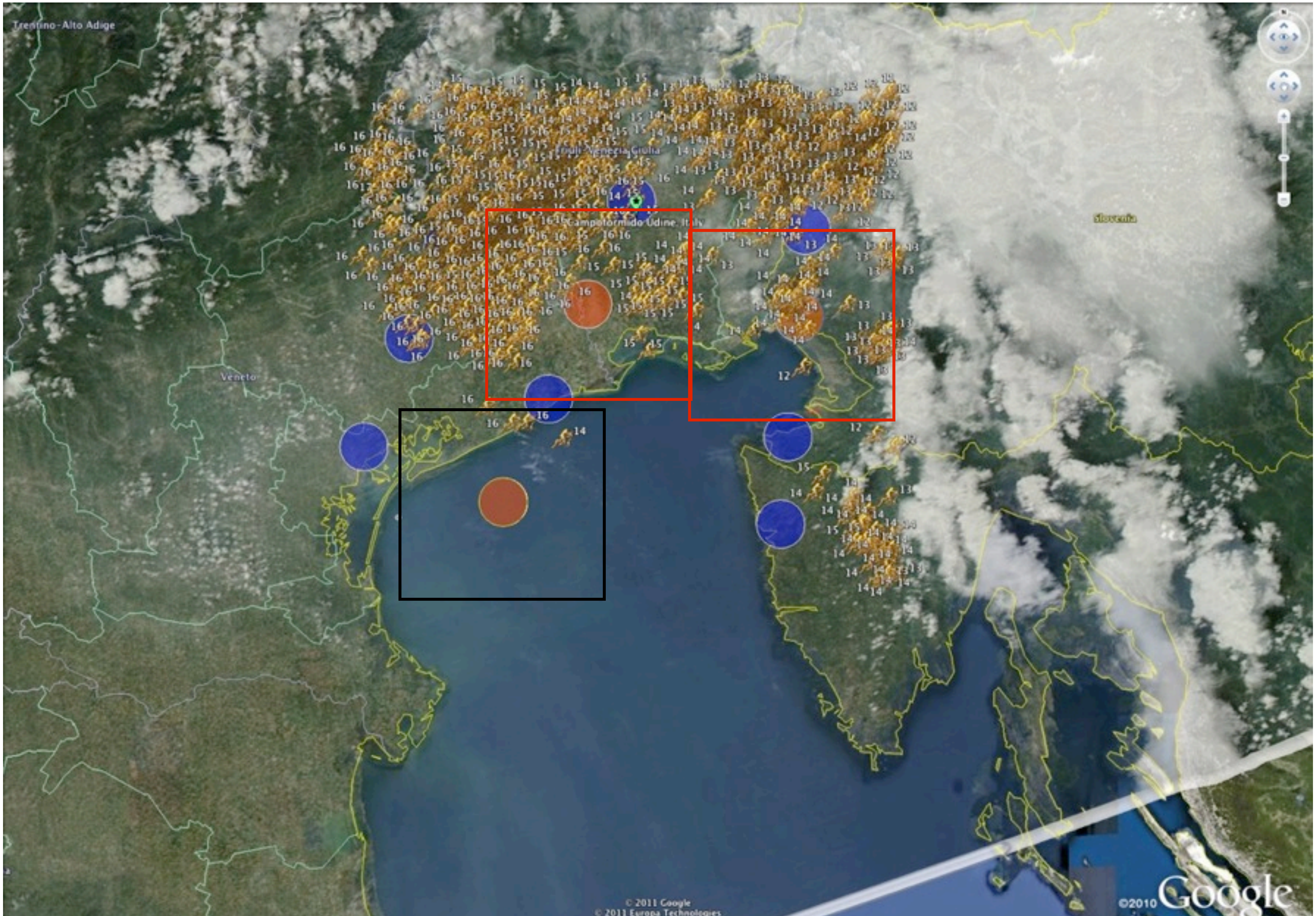

IASI Retrieval T

04 Oct 2009 09:05 UTC

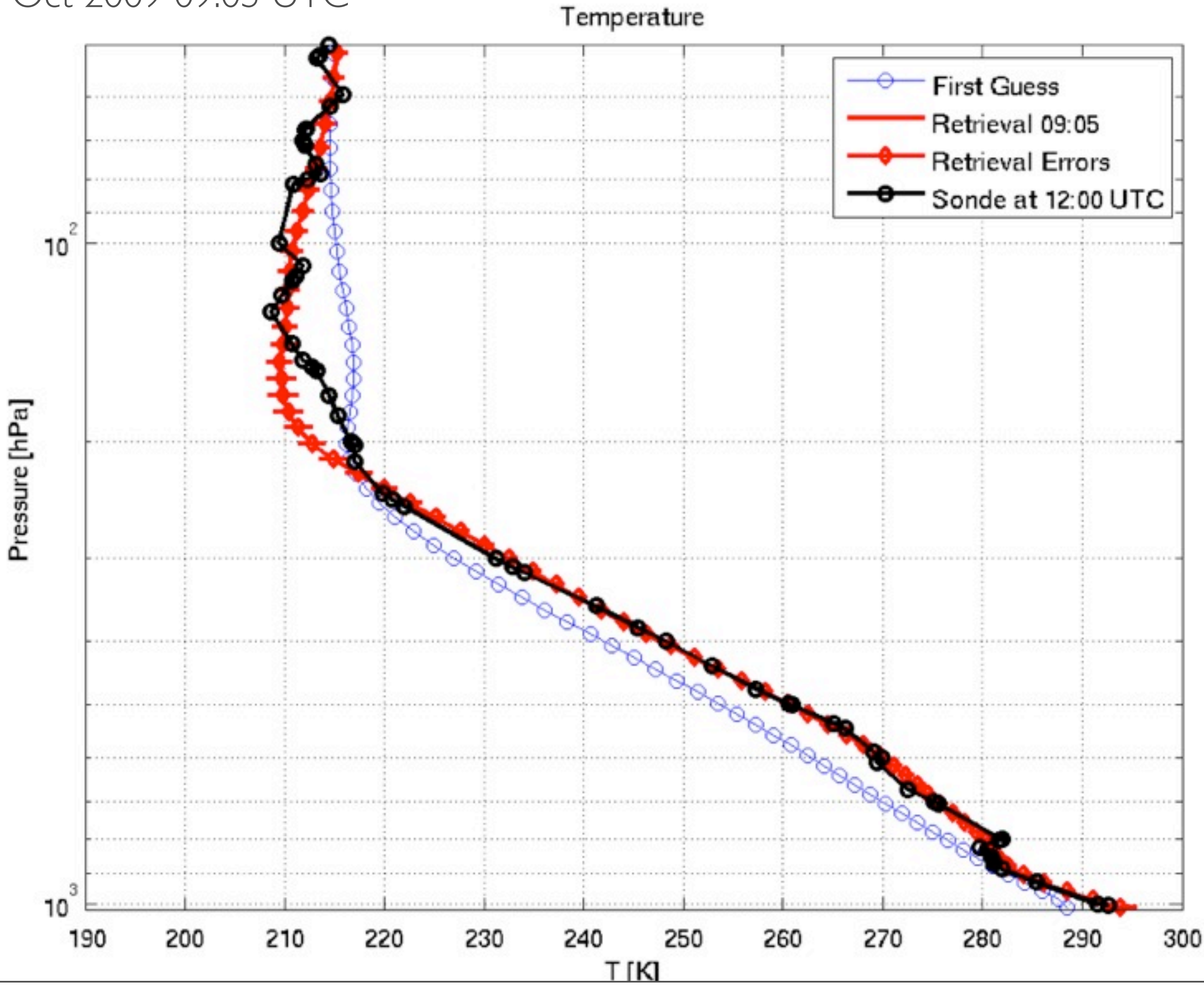

IASI Retrieval MR

04 Oct 2009 09:05 UTC

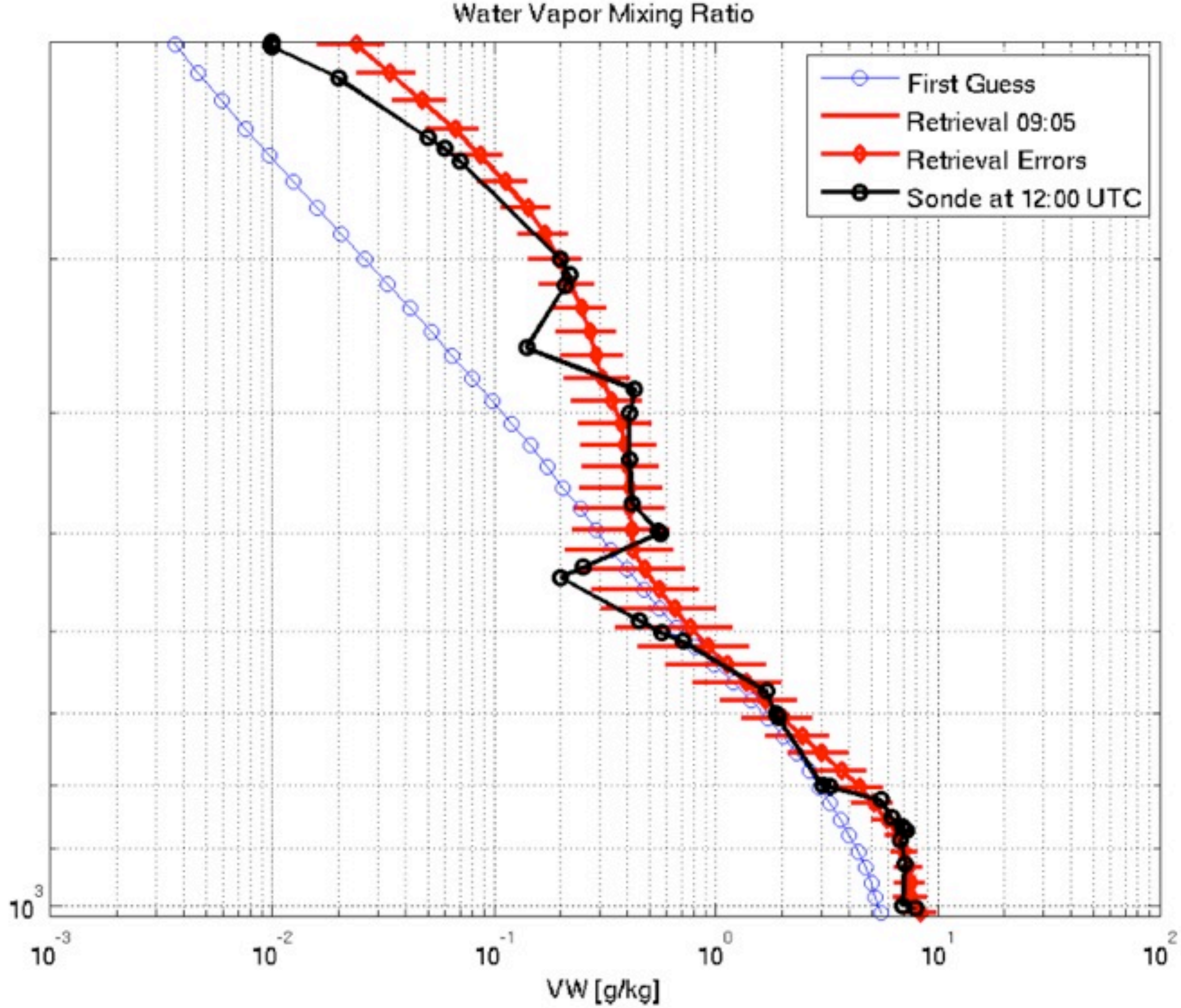

AIRS Retrievals T

Phase II | Improvements

03 April 2007 Temperature

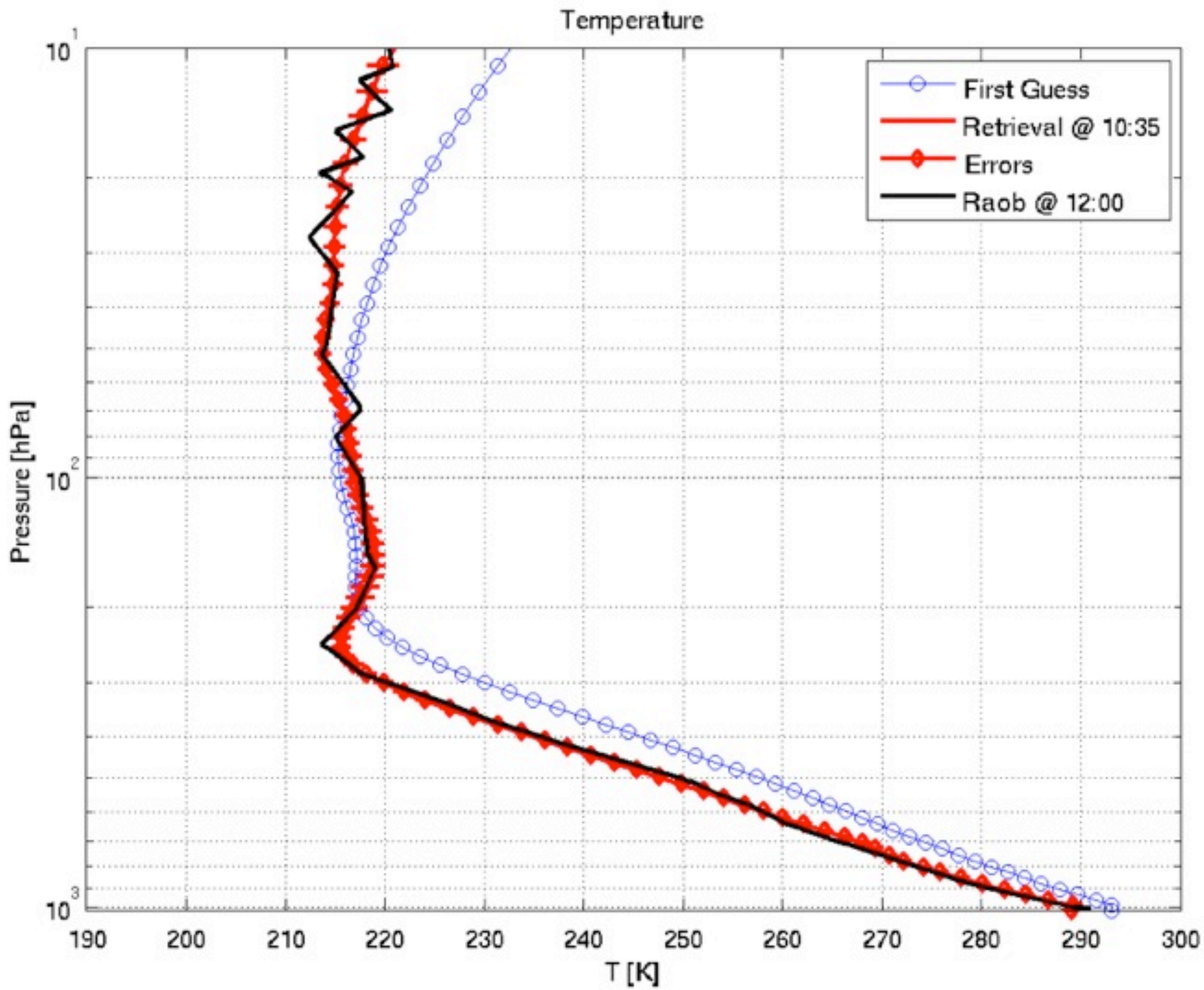

AIRS Retrievals MR

Phase II

Improvements

03 April 2007 Water Vapor Mixing Ratio

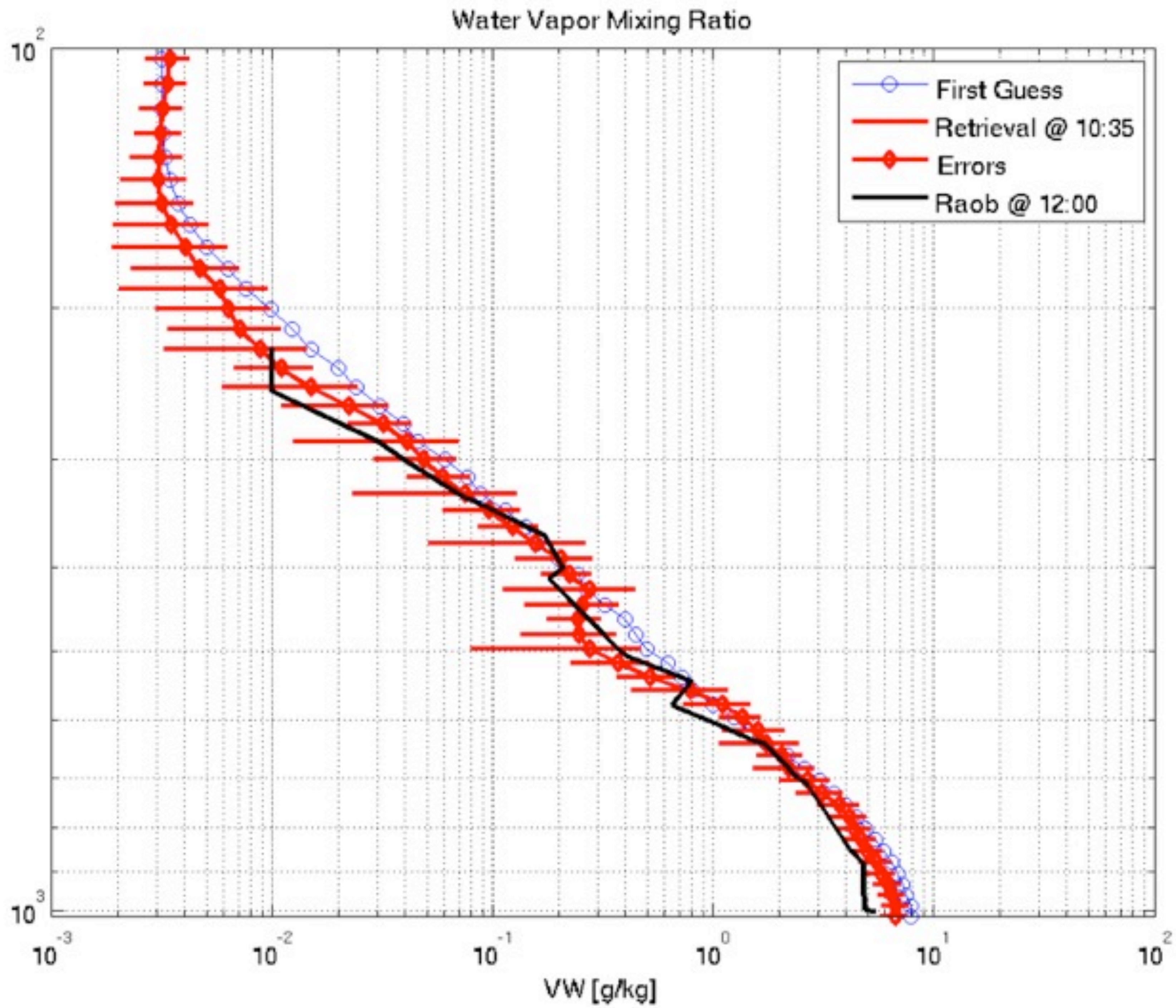

Conclusions

- New experiment ready to be performed with:
    - IASI and Linet data over Udine, Milano, Ajaccio, Nimes;
    - IASI and Euclid data over Udine;
    - AIRS and Euclid data over Udine;
- Retrieval quality is still in improving phase (long way to go);
- Number of available events substantially increased (order of thousand of retrievals available);
- First results over Udine available in about 30 days.

Conclusions

- New experiment ready to be performed with:
  - IASI and Linet data over Udine, Milano, Ajaccio, Nimes;
  - IASI and Euclid data over Udine;
  - AIRS and Euclid data over Udine;
- Retrieval quality is still in improving phase (long way to go);
- Number of available events substantially increased (order of thousand of retrievals available);
- First results over Udine available in about 30 days.

Very difficult to improve quality of LEVEL 2 products if they are not used.

Please join the effort presented by Stephen Tjemkes (Intercomparison of retrieval codes for hyperspectral infrared sounding observations)

Some references

Agostino Manzato, G. Morgan Jr. 2003: Evaluating the sounding instability with the Lifted Parcel Theory. Atmospheric Research 67–68 (2003) 455–473.

Agostino Manzato, 2001: A climatology of instability indices derived from Friuli Venezia Giulia soundings, using three different methods Atmospheric Research 67–68 (2003) 417–454

Agostino Manzato, 2001: A Verification of Numerical Model Forecasts for Sounding-Derived Indices above Udine, Northeast Italy Weather Forecasting (2007) 477–495

S. Puca, F. Zauli, L. De Leonibus, P. Rosci, and P. Antonelli 2009. Automatic detection and monitoring of convective cloud systems based on geostationary infrared observations. Submitted to Meteorological Applications, 2009.

Silvia Puca, Daniele Biron, Luigi De Leonibus, Paolo Rosci, and Francesco Zauli 2005. Improvements on numerical "objects" detection and nowcasting of convective cell with the use of seviri data (ir and wv channels) and numerical techniques. In The International Symposium on Nowcasting and Very Short Range Forecasting (WSN05), 2005.C.

Rodgers 2000: Inverse Methods for Atmospheric Soundings. World Scientific.

Some references

David Tobin, Paolo Antonelli, Henry Revercomb, Steven Dutcher, David Turner, Joe Taylor, Robert Knuteson, and Kenneth Vinson, 2007: Hyperspectral Data Noise Characterization using Principle Component Analysis: Application to the Atmospheric Infrared Sounder. J. Appl. Remote Sens. 1, 013515 (2007) doi: 10.1117/1.2757707

Antonelli P., H. E. Revercomb, W. L. Smith, R.O. Knuteson, L. Sromovsky, D.C. Tobin, R. K. garcia, H. B. Howell, H.-L. Huang, F.A. Best, 2004: A Principal Component Noise Filter for High Spectral Resolution Infrared Measurements. J. Geophys. Res.,109, D23102, doi: 10.1029/2004JD004862.

Huang H.-L., P. Antonelli, 2001: Application of Principal Component Analysis to high resolution infrared measurements compression, and retrieval. *J. Appl. Meteor*., 40:25, pp. 365-388

Turner, D.D., R.O. Knuteson, H.E. Revercomb, C. Lo, and R.G. Dedecker, 2006: Noise reduction of Atmospheric Emitted Radiance Interferometer (AERI) observations using principal component analysis. *J. Atmos. Oceanic Technol.*, 23, 1223-1238.

Swets, J. A., 1973: The relative operating characteristic in psychology. Science, 182, 900–1000.

Some references

A. Manzato, 2007: A note on the Maximum Peirce Skill Score. Weather and Forecasting, Vol 22, 5, pp. 1148-1154